Virtual Reality (2025) 29:94
https://doi.org/10.1007/s10055-025-01160-x

ORIGINAL ARTICLE

Machine learning-guided high-definition transcranial direct current stimulation prevents cybersickness

Alexander Hui Xiang Yang[1,2] · Cristian Galán-Augé[3] · Nikola Kirilov Kasabov[4,5,6,7] · Yusuf Ozgur Cakmak[8,9,10,11,12]

Received: 16 September 2024 / Accepted: 30 April 2025

Abstract

Extended reality (XR) environments, such as simulators, augmented reality, and virtual reality are major techniques in contemporary AI and entertainment systems. Cybersickness (CS) is a motion-sickness experienced by many users of XR. CS causes debilitating nausea, disorientation, and oculomotor issues. Treatment and prevention for motion-sickness typically involves drugs with sedative properties that impair task performance. These drugs are non-specific to CS and counter intuitive for enabling activity within XR. Our paper finds that there are specific spatiotemporal patterns of brain activity in certain functional networks related to CS and offers a method for the analysis of these patterns. The method can predict CS ahead of its onset and most importantly it suggests what intervention to apply in order to prevent CS in individuals. We apply a novel approach to CS prevention by using our previously developed spiking neural network (SNN) method, which can predict CS using electroencephalogram (EEG) pre-VR usage, before applying neuromodulation to disrupt CS-related functional networks in the brain. This approach provides an additional layer of screening before intervention with high-definition transcranial direct current stimulation (HD-tDCS). The study recruited healthy CS susceptible participants (9 male, 10 female, n = 19, 18–36 years old) and used a within-subjects design. EEG (32-channel, 10–10-configuration) was monitored at seated-rest and processed through the SNN for CS prediction. Immediately following a positive prediction, either sham, anodal or cathodal HD-tDCS was applied at the Cz area (5-min, 1.5 mA, 30 s-ramp-up/down) with subsequent 10-min VR immersion to record CS events. Main results: Cathodal stimulation yielded a significantly higher number of successful preventions compared to anodal (*$p = 0.01$) and sham (***$p = 0.00056$), achieving a large effect size (> 0.8) with a 47% reduction in CS likelihood. Significance: The treatment was hypothesized to work through disruption of activity at the motor processing and planning regions under Cz. The area appears to be a marker of ongoing CS susceptibility, and also a contributor towards the condition.

Keywords Cybersickness · EEG · Transcranial direct current stimulation · Machine learning

✉ Yusuf Ozgur Cakmak
yusuf.cakmak@otago.ac.nz

1 Cakmak Lab, Department of Anatomy, University of Otago, Dunedin, New Zealand

2 Manabridge Ltd, Queenstown, New Zealand

3 Department of Brain Modeling, Neuroelectrics SL, AV. Tibidabo 47B, 08035 Barcelona, Spain

4 AUT, Auckland University of Technology, Auckland, New Zealand

5 KEDRI, School of Engineering, Computer and Mathematical Sciences, Auckland University of Technology, Auckland, New Zealand

6 Institute for Information and Communication Technologies, Bulgarian Academy of Sciences, Sofia, Bulgaria

7 Dalian University, Dalian, China

8 Department of Anatomy, Cakmak Lab, Dunedin, New Zealand

9 Centre for Bioengineering and Nanotechnology As Point-of-Care Technologies Theme Leader, University of Otago, Dunedin, New Zealand

10 Brain Health Research Centre, Dunedin, New Zealand

11 Centre for Health Systems and Technology, Dunedin, New Zealand

12 Medtech Core NZ, Auckland, New Zealand

Published online: 10 June 2025

1 Introduction

Extended reality (XR) encompasses a range of technologies including screen-based simulators, augmented reality (AR), mixed reality (MR) and virtual reality (VR) (Adriana Cárdenas-Robledo et al. 2022). XR has diverse applications across entertainment, art, education, business, social, professional endeavours, health and defence (Ball et al. 2021; Cipresso et al. 2018). A key differentiator among XR technologies is the degree of immersion, which refers to the extent to which a system can engage users in an artificial environment. While VR provides a fully immersive experience, AR offers only partial immersion, overlaying digital elements onto the real world (Mauri et al. 2024). The level of immersion plays an important role in user experience, influencing factors such as telepresence—the sense of "being there" in a virtual environment—and embodiment, which refers to the feeling of ownership and control over a virtual body (Kim et al. 2023). Despite advancements, adverse physiological interactions during immersion remain a significant challenge, limiting the ergonomic and effective usage of XR (Caserman et al. 2021). Immersion into extended reality (XR) environments can cause a type of motion sickness called cybersickness (CS) in 60–95% of people. CS induces nausea, disorientation and oculomotor issues. Though temporary, these symptoms are sometimes severe enough to cause individuals to exit their immersion (Caserman et al. 2021). Some studies report a 5–13% abandonment rate in VR experiments (Caserman et al. 2021; Sharples et al. 2008; Stanney et al. 2020), while others see rates of 50% (Dennison et al. 2016; Martirosov et al. 2022). These issues have largely been mitigated through design best practices in modern XR, such as optimizing embodiment and presence using avatars and visual cues for body positioning, as explored in both industry (e.g., Meta) and research (Souchet et al. 2023; Kim et al. 2023; Makani et al. 2024). However, individual susceptibility remains a persistent challenge particularly for those who are highly prone to CS. For clarity, mentions of CS will relate specifically to visually induced motion sickness (VIMS).

Given that CS is a type of motion sickness, in special cases one may look towards drug treatment targeting motion sickness itself, but this solution presents a number of considerations (Koch et al. 2018). First generation antihistamines used in the prevention and treatment of motion-sickness can involve sedative properties that impair task performance (Leung and Hon 2019), compounding the fatigue already present in CS (Rebenitsch and Owen 2016). Furthermore, non-sedating second-generation antihistamines such as cetirizine, fexofenadine, astemizole and loratadine have been found ineffective for the prevention or treatment of motion-sickness (Brainard and Gresham 2014; Cheung et al. 2003; Kohl et al. 1987; Leung and Hon 2019). In general, sedation would be a counter-intuitive approach towards enabling activity within XR, especially if the activity demands high performance. It is also not known how these drugs would train the body to withstand digital environments in the long-term (Leung and Hon 2019). More research is required on the effectiveness of drugs for this condition specific to the context of XR usage. Furthermore, the repeated drug use required to treat CS would not be ideal for long-term access to XR technologies (Galili et al. 2019; Kohl et al. 1987; Lee et al. 2003; Luetje and Wooten 1996; Noreen et al. 2021; Scheurer et al. 2008; Zheng et al. 2014). Thus, it would be prudent to explore other means of treatment for CS that allow for continued XR usage, especially prevention.

Non-invasive electrical stimulation on the brain provides a drug free approach to CS treatment (Karrim et al. 2017; Spinks and Wasiak 2011). Transcranial direct current stimulation (tDCS), which modulates neural activities using low-amplitude current, is a promising method (Woods et al. 2016). High definition tDCS (HD-tDCS) is a more spatially precise method of tDCS that uses multiple electrodes to constrain current spread to a smaller area (To et al. 2018). In this method, a polarity specific current is induced by the central electrode at the target site, and the surrounding electrodes act as 'return' electrodes. These return electrodes have weaker currents of opposite polarity that are thought to constrain the effects of the electric field under the central electrode to a smaller spatial area (DaSilva et al. 2015). tDCS is known as a reversible modulation used to modify behaviours as well as improve task performances and learning (Coffman et al. 2014). In a review on tDCS for performance enhancement in military environments, this treatment has shown promise in the areas of executive functioning, cognitive flexibility, attention, decision-making, and working memory (Feltman et al. 2019). Therefore, tDCS may also be useful to modulate other cognitive events such as CS (Krokos and Varshney 2021). Additionally, this approach may enhance comfort and performance in XR environments, aligning with previous findings where tDCS has been shown to improve embodiment, presence, and task performance in teleoperation settings (Cesari et al. 2024).

Brain stimulation has been trialed for multiple VR rehabilitation protocols (Cassani et al. 2020). In contrast, research into this treatment for CS is scarce. Cathodal tDCS at P3 (parietal cortex, superior parietal lobule/precuneus) with the return electrode at the left ear has shown promise in delaying nausea onset for both motion sickness (Arshad et al. 2015) and mild CS (Li et al. 2020). These effects were explained to work due to disruption of the complex and distributed vestibular network (Frank et al. 2014; Raiser et al. 2020; Smith et al. 2022). Although, a downside was that the same stimulation parameters at P3 also caused asymmetrical

modulation of the vestibular ocular reflex (VOR), a reflex that stabilizes gaze during head movement (Bronstein et al. 2015). In another study, cathodal tDCS at AF4 (prefrontal cortex) with Pz as the return electrode was targeted to affect spatial navigation and modulate effective connectivity during spatial navigation (Hampstead et al. 2014), but added benefits were also found in terms of decreased oculomotor and disorientation symptoms for CS compared to baseline (Langbehn et al. 2019). Another study used anodal tDCS at CP6 (temporal parietal junction) with Cz as the return electrode (Takeuchi et al. 2018). This configuration affected the cortical site responsible for multimodal integration of visual and vestibular information, and was found to ameliorate disorientation and postural instability (Takeuchi et al. 2018).

While these studies are promising, they do not directly target motion sickness or CS, as their cortical site selection is based on broader sensory processing and functional significance rather than a direct link to nausea and sickness (Smith et al. 2022). A more targeted approach considers CS as an emergent property of brain networks, guiding intervention site selection based on this understanding (De Ridder et al. 2014; Vanneste and De Ridder 2012; Voneida 1998). This perspective suggests the existence of a 'CS core' network, a minimal set of brain areas jointly activated for CS occurrence, making it an ideal target for neuromodulation.

Therefore, there is a strong rationale for developing targeted tDCS interventions to mitigate CS, particularly for highly susceptible individuals. Such an approach extends beyond pharmacological treatments and design optimizations, which, while beneficial, may be insufficient in addressing CS in all cases.

Building on our previous work, we established a foundation for CS prediction using interpretable machine learning and knowledge discovery. Through spiking neural network (SNN) feature extraction, we identified Cz—an EEG electrode site located at the vertex of the head—as a crucial hub in CS network dynamics. Cz exhibited activity both at resting baseline and during CS events, predicting CS occurrence with 75% accuracy. Its strong correlation with CS emergence and susceptibility makes it a compelling target for neuromodulation-based CS prevention (Yang et al. 2023). Furthermore, our previous findings pinpointed specific EEG channels as key biomarkers for CS prediction. In this study, we extend that work by functionally testing whether modulating neural activity at Cz directly influences the onset of CS. Rather than solely validating our model's ability to generalize across participants, we experimentally probe the neural mechanisms underpinning CS susceptibility, assessing whether the biomarker identified by the model plays a causal role in CS emergence.

To explore this, we employed a machine learning-guided approach to CS prevention, using the same predictive model with Cz as a central hub. We predicted CS occurrences and evaluated the preventative efficacy of neuromodulation at this site. Our null hypothesis posited that neither cathodal nor anodal HD-tDCS would yield a higher number of successful treatments than sham stimulation. We introduced opposite polarities as an active control, and aimed to determine whether anodal or cathodal stimulation at Cz would be effective at influencing the occurrence of CS. Additionally, we conducted pattern analysis and simulated head models to assess the effects of stimulation, providing insights into information flow correlated with CS resistance. Collectively, these methods deepen our understanding of CS network dynamics, informing future neuromodulation-based interventions.

2 Methods

2.1 Recruitment

This study utilized a within-subjects double blind randomized interventional design. The study recruited 19 healthy participants (9 male, 10 female, aged 18–35 years old) with one dropout due to usage of psychoactive medication. The sample size was an optimistic estimate given a priori sample size calculations to achieve a power of 0.95 with an effect size of 0.95 at an alpha error probability of 0.05.

The intention was to capture a wide range of ages for generalizability to a large demographic. Incidence of motion sickness declines past the age of 50 (Schmäl 2013). Previous studies using EEG to classify CS have been conducted with ages ranging from 18 to 34 years old (Tauscher et al. 2020), and studies on functional connectivity during VIMS used ages ranging from 18 to 36 years old. Given this information, an age range of 18–35 was chosen.

The inclusion criteria were without prior neurological, cardiovascular, gastrointestinal disease, and not on regular medication or drugs. Inclusion was further restricted only to those susceptible to CS. This was achieved via two filters, a score of 10 or above on the VIMSSQ (Golding et al. 2021) and eligibility for treatment on the day of the session via a positive prediction for CS using the previously developed 75% accuracy prediction algorithm. This served to improve the reliability of treatment outcomes to prevent or alleviate CS.

The exclusion criteria included: implanted devices, head implants containing metal (outside of mouth), head wound, skin condition on scalp, previous adverse reactions to tDCS, pregnancy.

2.2 Questionnaires and scales

The following questionnaires and scales were used in the study:

2.2.1 Visually induced motion sickness questionnaire: 6 item (VIMSSQ)

Items are scored 0 (Never) to 3 (Often). A total scale score is formed by the addition of all items giving a maximum possible range for the VIMSSQ total scale score of minimum of 0 to maximum of 18. Higher scores indicate a stronger susceptibility to VIMS. The VIMSSQ is meant to be used in conjunction with the MSSQ (Golding et al. 2021), but a previous assessment of MSSQ-short scores (Yang et al. 2023) showed that there was no statistical difference between control and cybersick participants, and that distributions of MSSQ-short percentiles were similar. Thus, the VIMSSQ was used with a minimum cutoff score of 10/18, with the reason being that it equates to at least some previous experience of CS symptoms while using visual displays (Golding et al. 2021). The content of the VIMSSQ is available in Appendix 1.

2.2.2 Simulator sickness questionnaire (SSQ)

The SSQ is a well validated gold standard questionnaire that consists of a checklist of 16 symptoms rated based on severity of symptoms, and has the added advantage over that of the FMS to group oculomotor, disorientation and nausea symptoms (Kennedy et al. 1993).

2.2.3 Fast motion sickness scale (FMS)

The fast motion sickness scale can cover more minute differences in CS severity than the SSQ which has a 4-point scale. This 20 point scale is validated and used in other CS studies to report CS verbally (Keshavarz and Hecht 2011; Martin et al. 2020). This scale also has a strong correlation with the gold standard SSQ (Kim et al. 2023). The scores from this scale were compared between post-stimulation and during VR immersion and used as the primary outcome for analysis to determine treatment success.

2.2.4 Virtual reality sickness questionnaire (VRSQ)

The VRSQ is an extension of the SSQ (Kim et al. 2023). It is used as an adjunct to the SSQ in this study, to get a more specific scoring related to virtual reality environments. The VRSQ scores only the disorientation and oculomotor components, and the content and scoring are available in appendix 2.

2.3 Experimental procedure

The entire experiment design flow is summarized in Fig. 1.

2.3.1 EEG recordings

EEG was recorded for 2 min during algorithmic prediction, 2 min during the post-stimulation stage and for 10 min during the VR immersion.

2.3.2 HD-tDCS placement

The central electrode was Cz, with surrounding electrodes of opposite polarity at FC1, FC2, CP1, CP2, according to the 10–10 EEG configuration system. Stimulation consisted of 1.5 mA with a 30 s ramp-up/down. The stimulation intensity was chosen to match studies using 1.5 mA which had previous promise in ameliorating motion sickness and virtual reality sickness (Arshad et al. 2015; Takeuchi et al. 2018; Li et al. 2020). A consensus study shows that this is well below 4 mA safety thresholds (Bikson et al. 2016), with common

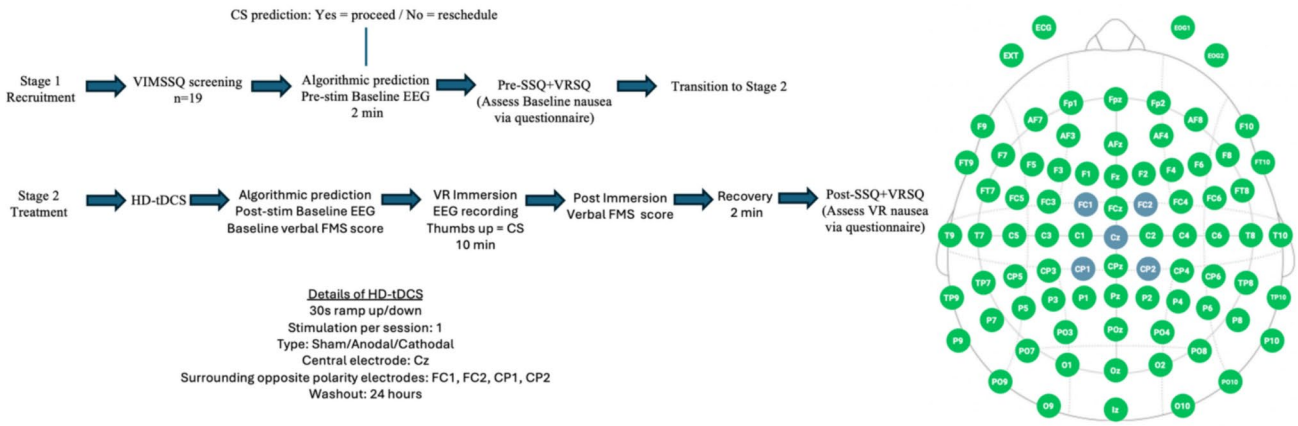

Fig. 1 Experiment design flow. Blue circles in the diagram indicate the location of electrodes

minor adverse effects ranging from sensations of itching, tingling, headache, burning and discomfort (Brunoni et al. 2011). Participants were asked to report any of these sensations after the experiment or subjectively abnormal reactions to the stimulation immediately to ensure safety.

2.3.3 VR video

The VR video played in the VR immersion and its ground truth nausea ratings have been published and created by researchers from Stanford University (Padmanaban et al. 2018). The video has also been used in our previous study as a stimulus to induce CS (Yang et al. 2023). The details of the VR video are available in the original publication and refer to a 'dotsinner.mp4', and are also shortly described here (Padmanaban et al. 2018). The video consisted of a random dot kinematogram (RDK), where dots were uniformly distributed in depth from 0.75 to 10 m and randomly positioned in angle. The chosen depth range helped minimize vergence–accommodation conflict, ensuring that the virtual image distance remained approximately 1.3 m. The participants were in a fixed head position looking forwards, the dots viewed rotated about the roll axis in a clockwise direction. To balance the depth distribution, foreground dots were placed between 0.75 and 5.375 m, while background dots ranged from 5.375 to 10 m, so that both sets had equal depth ranges and an equal number of dots. Each dot was sized so that it subtended the same visual angle, meaning the only available depth cue was binocular disparity. This meant that the kinematogram primarily allowed for stereoscopic depth perception and depth ordering, rather than other depth cues.

2.3.4 Experiment design flow

Participants were first assessed for inclusion into the study based on pre susceptibility to sickness via the VIMSSQ, passing if the score was 10/18 or above. On the day of each session, participants completed stage 1, a 2-min baseline recording prior to VR usage which predicted whether they would have CS or not. Their data at 30–32 s baseline was processed by a method proposed by us, Yang et al. (2023), based on the NeuCube SNN architecture (Kasabov 2014 2018) which compared the neural maps of participants to our pre-trained model to determine if they would feel CS in VR. For more information on the inner workings of the model please refer to Yang et al. (2023). Participants with positive predictions for CS completed an SSQ and VRSQ questionnaire as an initial assessment of their current sickness status and transitioned to stage 2 preventative treatment. Participants that had a negative prediction, rescheduled for another session until they finished all three sessions. Positively predicted participants immediately transitioned to stage 2 of the experiment. This prediction served as an additional layer to screen for CS susceptibly on top of the VIMSSQ. In addition, it provided information for timely intervention.

During stage 2, participants underwent 5 min of offline tDCS stimulation, 1.5 mA, 30 s ramp-up/down, at Cz with surrounding electrodes of opposite polarity at FC1, FC2, CP1, CP2, according to the 10–10 EEG configuration system. Brain plasticity for this length of stimulation is less than half an hour but lasts the duration of VR immersion which is 10 min (Woods et al. 2016). This stimulation was either sham, anodal or cathodal. The sham stimulation consisted of an anodal polarity but only a ramp-up and then ramp-down was given at the start of the experiment. The reason for opposite polarities was to introduce a form of active-control.

After stimulation, a 2-min post stimulation interim period was given prior to VR immersion, which mimics the 2-min baseline at the beginning. At the end of this period participants verbally rated their initial sickness using the FMS from 0 to 20. Participants then proceeded to watch a VR video of rotating white dots for 10 min using an Head Mounted Display (HMD). During VR immersion, all new sensations of CS were signaled with a thumbs up and were recorded on the timeline. Immediately following the end of VR immersion, participants verbally rated their average sickness using the FMS. Verbal reporting may introduce noise into the EEG data not just in the time segment of reporting itself but for a few seconds after before the signal stabilizes again, therefore in this experiment's case it was used post VR immersion rather than in the middle of it. Subsequently participants underwent a 2-min recovery period post VR immersion. EEG was recorded throughout the entire experiment, with the exception of no simultaneous EEG recording during the stimulation segment because the signal was masked by the applied electrical current. All participants eventually completed all randomized stimulations, for a total of 3 sessions at least 24 h apart. This was to ensure a minimum washout period between stimulation sessions and to minimize fatigue. All experimental sessions were conducted while seated. After the experiment, participants completed a simulator sickness questionnaire (SSQ) to assess the severity of sickness in conjunction with a Post VR immersion sickness questionnaire (VRSQ) (Kim et al. 2023).

2.4 Equipment

Data was collected and stimulation was given using a hybrid EEG head cap from starstim32 using NG Pistim electrodes (π cm^2Ag/AgCl/gel electrode, radius 1 cm) with conductive gel and the Neuroelectrics cap, XL size. The reference electrode was placed on the lobe of the right ear. Blinding was

enforced using NIC2.0 (Neuroelectrics) HTC Vive HMDs were used for virtual reality.

2.5 Analysis

Questionnaire scores were analysed using repeated measures ANOVA. As CS represents a cluster of symptoms, we chose to focus specifically on nausea as the indicator of treatment efficacy. Comparisons between the effects of treatments was analysed via Fisher's exact test. Successful treatments considered to be low to no nausea were defined as number of CS instances ≤ 1 and FMS delta scores ≤ 5. FMS delta scores are defined as the difference between FMS reported at the end of the post-stim period, which is after tDCS but before VR immersion, and FMS reported post VR immersion. These thresholds were determined before conducting statistical analyses. This gave an indicator of any increase in nausea after VR immersion and minimized influences that may have come about from experimental conditions (e.g. tightness of EEG headcap, the electrical stimulation itself, etc.)

The reasons for the threshold definition of successful treatment using these ranges are as follows:

(1) FMS delta scores are subjective indicators of nausea levels which may vary between individuals, meaning that a 5/20 or a 1/20 may equate to the same severity.
(2) An FMS score of 5 or below indicates below the 25% percentile for scoring and was chosen above the SSQ because of its immediacy in reporting and specificity towards nausea.
(3) The rotating stars VR video was expected to induce concentration, oculomotor, and disorientation problems due to its nature. Yet, the task of recognizing these feelings as distinct events is more difficult than it is for the visceral feeling of nausea. Nausea can also be tracked immediately on the validated FMS scale.
(4) Multiple instances of reported nausea over the 10-min span of the VR video were regarded as an indicator of unsuccessful treatment. A VR user should not be bombarded constantly with new nauseogenic experiences, even if severity levels are low.

2.6 Simulated head model for tDCS effects

A simulated head model was constructed to map and analyze the electrical field distribution across an averaged cortical surface, providing insight into the simulated response of large neuronal populations to the tDCS protocol used in this study. The mechanisms of tDCS are known for pyramidal cells, but the role of other types of neurons, such as basket cells (interneurons) or glia, are still not well understood. For a long, straight finite fibre with space constant λ in a homogeneous electric field, the transmembrane potential difference is largest at the fibre termination, with a value that can be approximated by $\lambda \cdot \hat{n}$, where $\hat{n}$ is the unit vector defining the fibre axis. This is an expected first-order result, with a spatial scale provided by the membrane space constant and directions by field and fibre orientation (Ruffini et al. 2014). Therefore, understanding the effects of tDCS requires knowledge of the spatial distribution of the generated electric vector field in the brain (Miranda et al. 2013).

The head model used in this study was created by using the software tool SimNIBS 3.0 (Thielscher et al. 2015) and custom Matlab scripts. The T1-weighted MRI was segmented by SimNIBS into scalp, skull, cerebral spinal fluid (CSF), grey matter (GM) and white matter (WM) masks using the default headreco pipline, which takes advantage of the SPM12 and CAT12 segmentation toolboxes. Models of PITRODE electrodes (cylinders, 1 cm radius) were placed in the scalp positions corresponding to the 10–10 EEG system. Tetrahedral finite-element meshes of the head and electrodes were created by SimNIBS using Gmsh (Geuzaine and Remacle 2009). Healthy brain tissue nodes were assigned electrical conductivity values appropriate to the DC-low-frequency electrical currents: 0.330 S/m (scalp), 0.008 S/m (skull), 1.790 S/m (CSF), 0.400 S/m (GM), 0.150 S/m (WM) (Miranda et al. 2013). The finite elements calculation for the E-field were performed by SimNIBS solving iteratively Laplace's equation for each bipolar electrode montage having Cz as a common cathode (−1 mA). The distribution of E_n for any montage involving these electrodes can then be calculated by summing the E_n distributions for each montage multiplied by the current in each electrode (Ruffini et al. 2014).

A standard head model based on Colin 27 (Copyright (C) 1993–2009 Louis Collins, McConnell Brain Imaging Centre, Montreal Neurological Institute, McGill University-Permission to use, copy, modify, and distribute this software and its documentation for any purpose and without fee is hereby granted, provided that the above copyright notice appear in all copies) average brain (stereotaxic average of 27 T1-weighted MRI scans of the same individual) was built. The montage is defined as follows for the Cz anodal conformation (for cathodal, current signs would be the opposite):

- Cz: 1.500 mA
- FC1: −0.375 mA
- FC2: −0.375 mA
- CP1: −0.375 mA
- CP2: −0.375 mA

The analysed area was defined as a circular area with a radius (R) varying from 1 to 6 cm in steps of 0.5 cm. The goal was to analyse the evolution of the average electric field (E_n) in

the region of interest ($< E_n^{Target} >$). The target region was set to excitation or inhibition and the rest of the cortical surface was set to no-stimulation, i.e. $E_n^{Off-Target}$= 0.0 V/m.

The parameters for simulation were the same used in this study for stimulation:
Stimulation type: tDCS
Target: Area below Cz electrode
Electrode type: PISTIM (π cm^{2}Ag/AgCl/gel electrode) (radius 1 cm)
Max current any electrode: 1.50 mA
Max total injected current: 1.50 mA
Max number of electrodes: 5
Other: Neuroelectrics cap, XL size.

2.7 EEG pattern analysis

For each participant, two SNN models were created and trained on data each at different time points using custom Python 3 software. Both models consisted of a 'reservoir' of 1471 leaky fire and integrate (LIF) neurons (Burkitt 2006) spatially mapped via Talairach coordinates, with input neurons mapped to their associated 10–10 EEG electrode positions (Koessler et al. 2009). In the reservoir, nodes are connected via small world connectivity, and their weights represent the magnitude of the frequency of firing activity as well as the degree of temporal synchronisation. The SNN therefore acted as a spatiotemporal data processing machine that extracts features by simulating interaction and spread of EEG activity from multiple input sites, producing distinct emergent patterns of activity. This differed from the simulated head model in that it simulates the interactions of EEG data instead of mapping expected electric field distributions induced by the stimulus. For more conceptual explanations of data processing machines refer to Kasabov et al. (2016) and Yang et al. (2023). The first model contained data from 30 to 32 s baseline, which is the same data used for their prediction of CS, and the second from 30 to 32 s post-stimulation. Initial connection weights were standardized to the previous study's CS template model, such that any change would capture different firing activity from multiple regions over time (Yang et al. 2023). Connection weights between timepoints (before and after cathodal stimulation) and nodes were tested for normal distribution using Shapiro-Wilk test, and for significance using paired T-test or non-parametric Wilcoxin Signed-Rank test depending on the distribution of data for each node. Connection weights from the baseline timepoint were subtracted from the post-stimulation timepoint and only the significantly different nodes were kept for visualisation. The learning rule for updating connection weights consisted of a form of spike timing dependent plasticity (STDP) (Feldman 2012) which reinforced weights between presynaptic and postsynaptic nodes to encourage more firing. The equation for the learning rule was as follows:

$$W_{pre,post} = \begin{cases} W_{pre,post} + C & if\ causal\ or\ synced \\ W_{pre,post} - C & otherwise \end{cases} \quad (1)$$

where W is the connection weight between a presynaptic and postsynaptic node, and C is a coefficient that adds to the propensity of a neuron firing, such that it further strengthens frequently used pathways of signal flow and encourages temporal synchronisation of firing.

Table 1 Predictions correlating with actual outcome per stimulation type, out of n = 19

Sham	Anodal	Cathodal
11 (57.9%)	16 (84.2%)	10 (52.6%)

3 Results

3.1 Post stim predictions

The algorithm was applied again in the post stim period to predict CS. It worked close to its validated accuracy (75%), with 68.4% of total predictions matching actual outcomes across stimulation types. Table 1 shows the breakdown per stimulation type.

3.2 Questionnaires

Differences from baseline in VRSQ scores, Total SSQ scores, Nausea, Oculomotor and Disorientation components between stimulations were not significant $p > 0.05$.

3.3 Other CS metrics

There were no significant differences between the sham, anodal and cathodal HD-tDCS treatments for number of CS instances or FMS delta scores. However, after applying our threshold definition for successful treatment, significantly more participants experienced low to no nausea after cathodal treatment compared to anodal ($p < 0.01$) and sham ($p < 0.001$) (Fig. 2). The following effect size results will focus on these significant findings.

3.4 Effect sizes

A thorough inhibition of CS (instances ≤ 1, FMS delta score ≤ 5) was observed in the cathodal condition (n = 9) compared to the anodal (n = 2) and control conditions (n = 0). The effect sizes are shown in Fig. 3. The Cohen's D of 1.40 when compared to sham, and 1.09 when compared to anodal treatments suggests a large effect size of

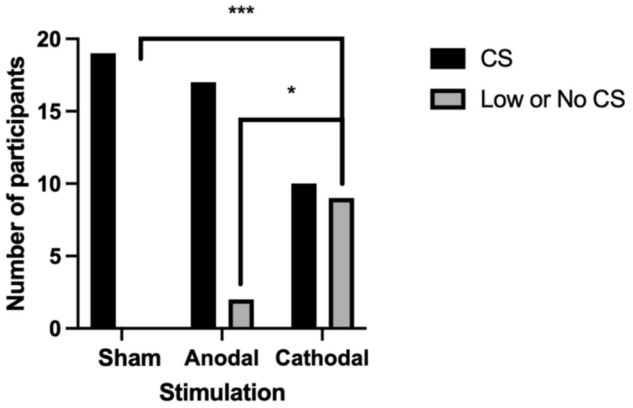

Fig. 2 Binary treatment outcomes between stimulation types. Cathodal stimulation yielded a significantly higher number of successful treatments (very light or absence of CS) than sham and anodal, *** indicates $p=0.00056$, * indicates $p=0.01$ with Fisher's exact test

the treatment and a strong impact on the reduction of CS, with 95% confidence intervals (CI) well within the range of a large effect size (0.8 and above) (Sullivan and Feinn 2012). However, anodal compared to sham had relatively low effect size (0.31, CI 0.04–0.58). Relative risk showed that CS is 47% and 41% less likely to occur after cathodal treatment than in sham and anodal conditions respectively. The odds ratio showed that the odds of developing CS after cathodal treatment is 0.06 times the odds for sham and 0.14 times the odds of anodal conditions, suggesting that cathodal treatment is associated with a much lower risk of CS. The confidence intervals were quite wide for odds ratio and relative risk, which brings to question the precision of these values. However, an exception is the odds ratio for cathodal/sham, which has a tight interval in comparison.

3.5 Biophysical stimulation montage

This section presents the evolution of $< E_n^{Target} >$ along the evaluated area. Distribution of the E_n are shown at Figs. 4, 5 and 6. Here, a logical decrease in absolute terms of the E_n can be observed as the regions are more distant from Cz and near to the return electrodes. To assess

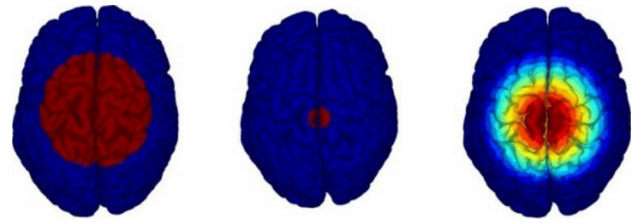

Fig. 4 Reconstruction of the cortical surface to display Cz stimulation effects. At left, the largest analyzed area corresponds to a circular area below Cz with a radius of 6 cm. In the middle, the minimum analyzed area with a radius of 1 cm. At right, the representation of the area in radial segments of 0.5 cm. Darkest blue means no stimulation while the other colours mean stimulation

the decreased trend, the $< E_n^{Target} >$ was evaluated by progressively increasing its size. In Fig. 5, both curves for anodal and cathodal montages are presented. The $< E_n^{Target} >$ value reaches the absolute maximum when $R=1.0$ cm ($< E_n^{Target} > = 0.044$ V/m). The ($< E_n^{Target} >$ presents a logarithmic decrease until reaching a value close to zero at $R=6.0$ cm ($< E_n^{Target} > = 0.003$ V/m). This curve presents a monotonic trend. Numerically, in Table 2, the ($< E_n^{Target} >$ drops almost to the 50% when $R=2.5$ cm (decrease of 48.15%) and it plateaus nearby R=4 cm.

At Table 2 together with Fig. 4 it can be observed that there is a quick decrease of $< E_n^{Target} >$, losing nearby 50% of the maximum value at $R=2.5$ and $R=4$ cm because the boundaries of the evaluated area are already nearby the return electrodes. Setting electrodes further away to Cz would allow for an overall larger $< E_n^{Target} >$ in the whole area but montage focality would decrease. The curve from Fig. 5 represents a monotonic trend but at $R=2.5$ cm there is a sudden change in the slope. This change is due to the anatomical features intrinsic to the evaluated area together with the distance between the evaluated area and the surrounding return electrodes, as is detailed in Salvador et al. (2021).

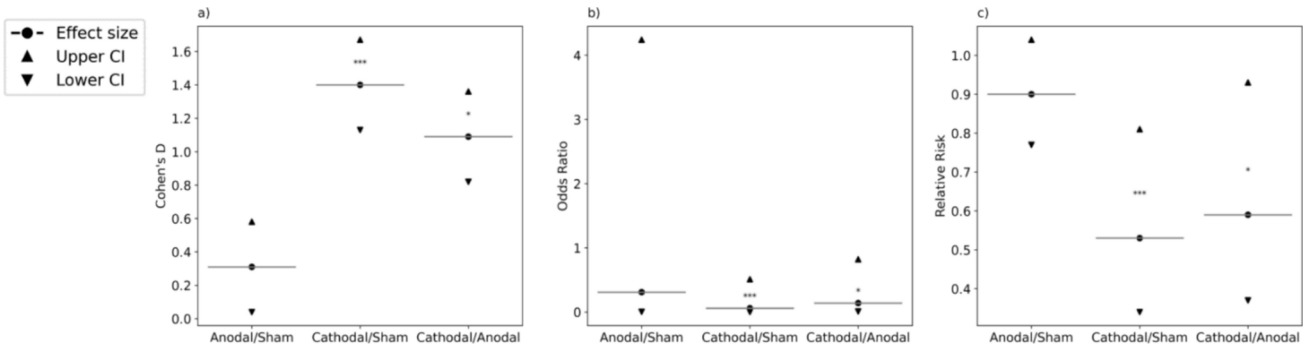

Fig. 3 Effect size statistics. Stars represent p values *** indicates $p=0.00056$, * indicates $p=0.01$ with Fisher's exact test

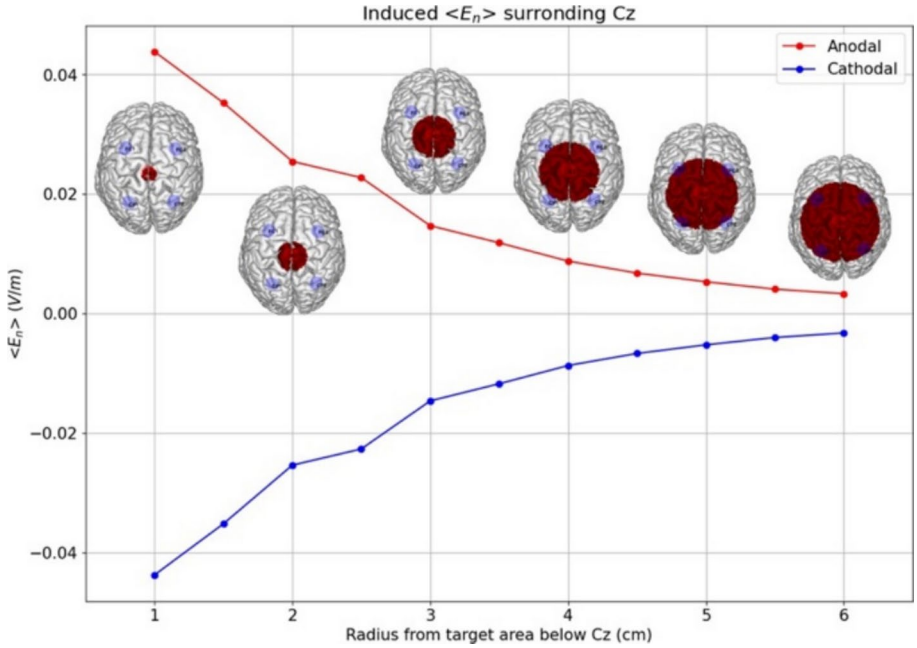

Fig. 5 The Electric field induced by Cz at increasing radius from electrode site. Resulting curves show an exponential decrease of the induced $<E_n>$ in the gray matter as the evaluated area becomes larger. Images of the brain are included for reference of the size of the assessed areas. From left to right: Area with $R=1$ cm, $R=2$ cm, $R=3$ cm, $R=4$ cm, $R=5$ cm, $R=6$ cm

3.6 SNN pattern analysis

Connection weights between nodes in the SNN reservoir signified the amount of firing activity between them, modulated by the synchronization and frequency of firing between node pairs. The simulated EEG pattern analysis (Fig. 7) revealed widespread and distributed changes in activity, mainly a decrease in activity from baseline after cathodal stimulation was applied. Only nodes, with significant differences (average p value = 0.01288) between baseline and post-stimulation were visualized.

4 Discussion

4.1 Cybersickness metrics

Application of cathodal HD-tDCS at Cz was associated with a significantly lower number of positive predictions post stim and reduced instances of CS compared to both sham and anodal HD-tDCS, suggesting that this may be a potential preventative treatment for the inhibition of CS. The results suggest that CS may arise from a change in brain activity under Cz related to motor processing and movement planning. Another study supports this polarity preference, showing that cathodal stimulation at the P3 site above the parietal cortex alleviates motion sickness but not anodal stimulation at the same region (Arshad et al. 2015). It is interesting to note that opposite polarities of stimulation did not have opposing effects, where it was expected that if cathodal stimulation prevents CS, then anodal stimulation might have worsened the effects of CS, but this was not the case. While cathodal stimulation compared to sham and anodal had high effect size (Cohen's D 1.40, 1.09 respectively), the lack of significant differences between anodal and sham conditions, coupled with the low effect size (Cohen's D 0.31) and large confidence interval (0.04–0.58) indicated that this specific result should be interpreted with caution. Future studies may need larger sample sizes to account for anodal stimulation effects. Nonetheless, anodal and cathodal tDCS at the same intensity have produced different outcomes across other areas of interest, for example in behaviour (Jacobson et al. 2012; Ostrowski et al. 2022) and in migraine (Rahimi et al. 2020). Another possible explanation for the lack of strictly opposing effects lies in the baseline excitability of the targeted brain region. Cathodal stimulation might be more effective at modulating excitability or boosting homeostatic functions in CS, whereas anodal stimulation—despite typically inducing opposite effects—might have a subtle enhancing effect but this may translate to a negligible impact on severity in individuals who are already predisposed to CS (Siebner et al. 2004; Bestmann et al. 2015; Fertonani and Miniussi 2017). Research suggests that the effect of tDCS depends on initial cortical excitability (Siebner et al. 2004; Bergmann 2018). Moreover, tDCS effects can be nonlinear, meaning anodal stimulation does not always enhance excitability nor does cathodal stimulation always suppress it (Batsikadze et al. 2013). These effects can also be intensity dependent, as different current strengths may paradoxically reverse expected outcomes (Batsikadze et al. 2013). It was not known how changes in brain activity in this area might affect task performance as the experiment was relatively passive and did not require active engagement with the VR environment.

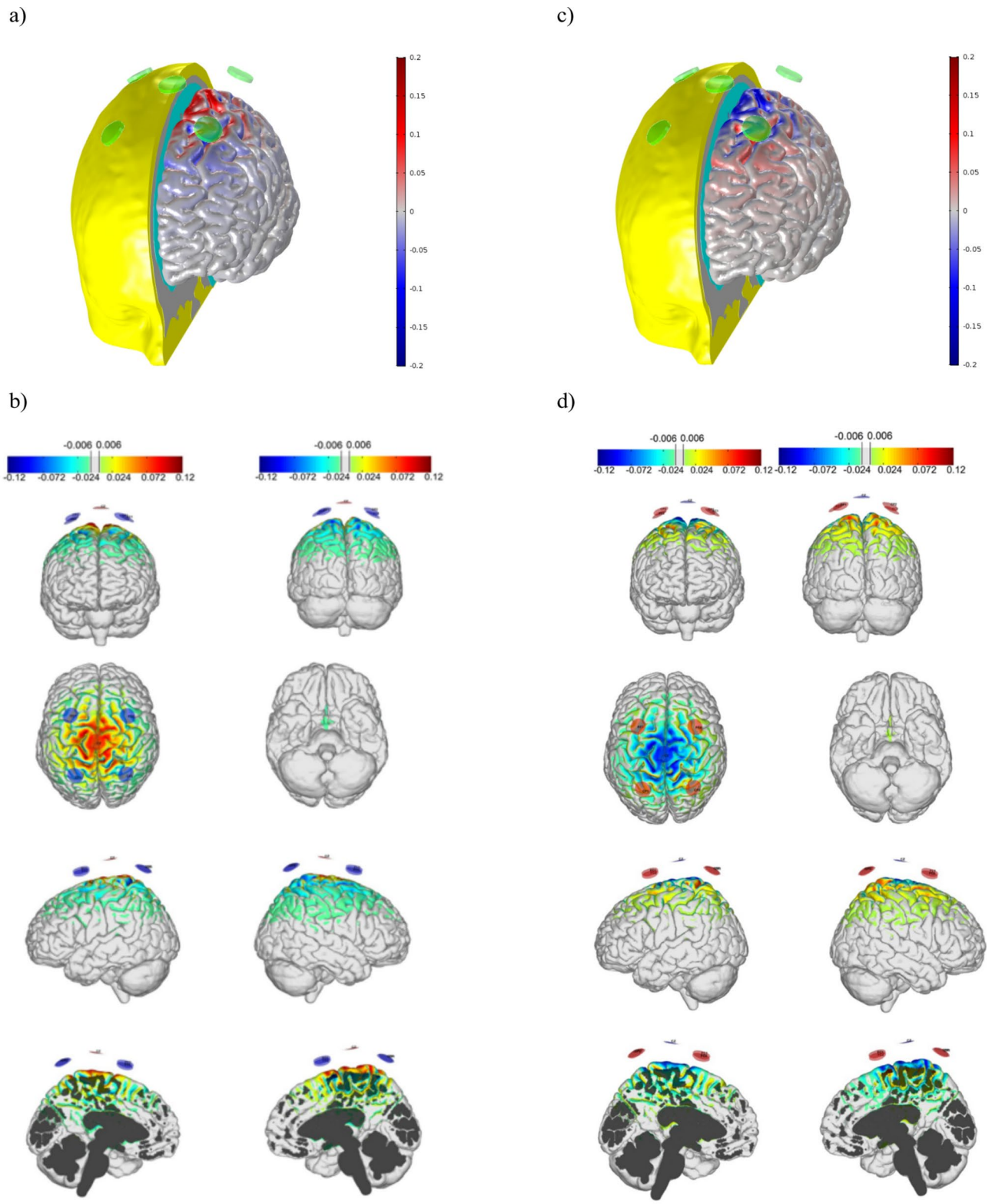

Fig. 6 Electric field induced by Cz as anodal electrode (excitation) in **a** and **b**, and as cathodal electrode (inhibition) in **c** and **d**. The map corresponds to the normal component of the E-field En (V/m). The majority of the E-field is applied at the cortical surface, and a smaller amount traverses deeper. The skin is represented in yellow, the skull in gray, and the CSF in cyan

Table 2 $< E_n^{Target} >$ per *R* value and montage

Radius (R) (cm)	Anodal $< E_n^{Target} >$(V/m)	Cathodal $< E_n^{Target} >$(V/m)	Decrease relative to maximum (%)
1	0.044	− 0.044	0.00
1.5	0.035	− 0.035	19.55
2	0.025	− 0.025	41.96
2.5	0.023	− 0.023	48.15
3	0.015	− 0.015	66.52
3.5	0.012	− 0.012	73.07
4	0.009	− 0.009	80.04
4.5	0.007	− 0.007	84.65
5	0.005	− 0.005	87.95
5.5	0.004	− 0.004	90.76
6	0.003	− 0.003	92.51

Deeper structures were also reached according to the head simulation model such as the mid cingulate cortex (MCC). During visually induced nausea, this area was found to have increased connectivity to the left V5/MT, which is involved in priming for motion direction (Toschi et al. 2017). The study provides support for the use of preventative tDCS to resist CS in VR and points the way for future research into possible interventions. The neuromodulation may work both by affecting the activity in the regions under Cz and by disruption of the network responsible for CS, thereby restoring 'normal' brain function. This suggests not only a connection between movement processing and the development of CS but also that regions beneath Cz may have additional roles in facilitating information flow within a CS brain network. Overall these findings further support the role of the brain regions beneath Cz as a key hub in the neural processing of CS, building upon our previous study, which identified Cz as a critical site for both CS susceptibility and emergence (Yang et al. 2023). However, although application of HD-tDCS at the Cz electrode site led to the observed effects, the definite contribution of areas under Cz remains speculative, as discussed further directly below.

4.2 Offshoot effects

One point to note is that the surrounding electrodes in HD-tDCS with opposite polarities could have had local and distant effects from the electrode sites (Thair et al. 2017), thereby affecting more regions than just those directly under Cz. Thus, it is difficult to pinpoint the exact mechanism that would explain these findings and future research is needed on this area. Furthermore, for regions beyond the electrode, the modulation induced can be the same or opposite to the stimulation's polarity (Thair et al. 2017). In the case of HD-tDCS on Cz which enhances focality, it is not yet known how this may affect the CS related network to disrupt CS. However, the results of the stimulation montage model shows a simulation of the effectiveness of HD-tDCS to spatially constrain the E-field to the target area.

4.3 Questionnaires

The lack of significant differences on average between stimulation types in SSQ and FMS scores, but a clear preventative effect for the cathodal treatment suggests that comparing averages of raw scores alone could not be reliable to differentiate between experimental conditions. In addition, it is possible that the baseline SSQ and post-stimulation SSQ values may not be comparable. Yet, taking the difference between the two seems to be the best method so far as 'zero baseline assumptions' have been considered erroneous (Brown et al. 2022). These false assumptions likely extend to the VRSQ (Kim et al. 2023), which is an extension of the gold-standard SSQ that applies a calculation to only the oculomotor and disorientation component. Another point is the nature of subjectivity for SSQs, in that the exact same perception could yield a different score between two people.

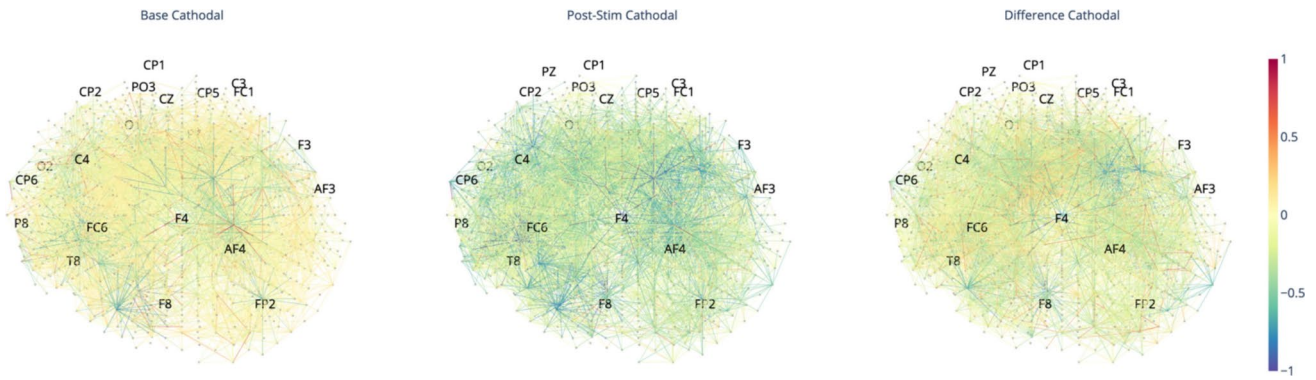

Fig. 7 Pattern analysis displaying the result of recorded EEG activity simulated in an SNN model. Baseline, post-stimulation and the difference between the two are shown for the cathodal condition. Areas with red indicate higher activity, areas with blue indicate lower activity

4.4 Knowledge discovery via SNN

The connectivity of the brain is a complex interplay between different areas and their functions, and activity in one area can have an impact on perception. While cathodal stimulation of Cz is effective in reducing CS, it may also affect other areas of the brain and perception. The pattern analysis of EEG activity in the SNN in Fig. 7 shows that widespread plastic changes in the brain occur after stimulation and reveals that multiple regions of the brain may be responsible for a complex network involved in resistance to CS.

4.5 Sham protocols

The sham protocol was used in this study with the rationale that the strongest sensations would be felt during the first part of stimulation, and also that participants would be able to feel the sensation turning off at the end of stimulation. The only adverse sensations reported to be felt during this experiment was tingling (Brunoni et al. 2011). This traditional ramp-up/down method has limitations; although currents are ramped down after a short time, cortical effects may still be induced. These possible cortical effects are an unfortunate trade-off for blinding and currently methods are scarce to prevent unwanted cortical effects (Koessler et al. 2009; Wallace et al. 2016). Recent research has suggested reducing cortical effects by maximizing current shunt through the scalp through electrode montage optimization (Dagan et al. 2018), although this still requires further investigation.

4.6 Limitations

The head model with simulated electric field distribution did not account for the presence of the HMD, which may have influenced the electric field distribution. In addition, individual differences in skull thickness, cerebral spinal fluid distribution and anatomical variability could influence how electric fields interact with the cortex, leading to variability in tDCS effects (Opitz et al. 2015). The prediction tool used in this study was validated at 75% accuracy, meaning that some participants may have received stimulation despite being incorrectly classified as susceptible to CS, potentially impacting the results. For instance, the effects of cathodal stimulation on individuals who were not truly susceptible to CS remain unclear and warrant further investigation. Additionally, this study focused on targeted intervention at the same hub as was used for prediction. However, there remains the possibility that on an individual level a subject may be susceptible to cybersickness but have different personalised markers at EEG baseline. In such cases a more personalised approach to intervention might be necessary. Although the sample size (n = 19) was statistically justified based on expected effect sizes and power calculations, it relied on optimistic effect size assumptions. Given this, the sample remains relatively small, and additional studies are necessary to confirm these findings. Furthermore, the random dot kinematogram (RDK) used in the VR video may not fully generalize to cybersickness across all XR experiences. This study assumes that cybersickness, regardless of the specific stimulus, results from common dysfunctions within key hubs of the CS network. In other words, it is unlikely that different stimuli and methods of inducing CS engage entirely separate neural hubs—though this remains an area for further research. Under this assumption, the type of visual or sensory stimulus is secondary to the underlying neural mechanisms responsible for the perception of sickness. This idea is supported by research identifying key perceptual hubs that contribute to various sensory experiences, including those involved in visual perception during action (Vega-Zuniga et al. 2025), olfactory perception (Jiang et al. 2022), and phantom auditory perception in tinnitus (Mohan et al. 2016). Nonetheless, further studies are needed to validate whether cathodal stimulation can mitigate CS across different types of stimuli. The use of tDCS at the intensity applied in this study is considered safe; but as this was an acute effects study, the chronic, metaplastic and plastic effects of stimulation over the long term need further research (Brunoni et al. 2011; Hulme et al. 2013; Bikson et al. 2016). Ergonomic implementation will depend on future advancements in headcap design and the broader acceptance of neuromodulation technologies (Lacko et al. 2017). A valuable takeaway from these findings could be the exploration of alternative neuromodulation strategies, such as neurofeedback, which allows individuals to train and regulate hubs within the CS network in a less invasive and more user-driven manner.

4.7 Future research

Several avenues remain open for future exploration. Alternative brain stimulation techniques, such as transcranial alternating current stimulation (tACS), may provide additional benefits. Li et al. (2021) identified an inverse relationship between CS severity and frontoparietal phase-locking, suggesting that in-phase tACS to the frontal-to-left-parietal network could stabilize neural oscillations and reduce CS susceptibility. Future studies could validate this approach and compare the effectiveness of tDCS, tACS, and other non-invasive neuromodulation techniques in modulating CS-related neural activity. Another promising direction is neurofeedback training, which could offer a less interventional, self-regulated approach to CS mitigation (Marzbani et al. 2016). Since our findings suggest that Cz activity is linked to CS resistance, future research could explore

whether real-time EEG-based neurofeedback enables individuals to train and regulate activity at Cz or other CS network hubs, particularly for frequent VR users, pilots, and military personnel. The long-term effects of neuromodulation on brain plasticity and CS resistance also warrant investigation. While this study demonstrates acute effects of tDCS, future research should explore whether repeated sessions induce lasting adaptations, optimizing tDCS treatment protocols for durability and effectiveness (Palmisano and Constable 2022; Shiravand et al. 2024). Personalized neuromodulation strategies may further improve efficacy, as individual differences in brain structure, baseline excitability, and CS susceptibility suggest that a one-size-fits-all approach may not be optimal (Opitz et al. 2015). Integrating real-time biomarker monitoring with adaptive machine learning-driven neuromodulation could enable personalized CS mitigation interventions. Beyond neuromodulation, combining tDCS with VR-based motion adaptation strategies could enhance CS resilience. Techniques such as reducing visual-vestibular conflict, optimizing frame rates, and dynamic field-of-view adjustments could work synergistically with neuromodulation to improve CS prevention (Souchet et al. 2023). Finally, hardware and ergonomic advancements remain an essential area of future research. While tDCS is considered safe at the applied intensity, optimizing headcap design and user acceptance is crucial for practical application (Lacko et al. 2017). The SNN-based predictive model developed in this study could also be optimized for real-time, low-power neuromorphic hardware, enabling on-the-fly CS detection and intervention in real-world XR environments (Ivanov et al. 2022).

5 Conclusion

This study presents a machine learning-guided neuromodulation approach for CS prevention, demonstrating that Cz is not only a predictive biomarker but also a site where neural activity can be modulated to enhance CS resistance. This finding suggests that information arising from Cz—and possibly underlying brain regions—can be leveraged for targeted interventions, providing new avenues for CS mitigation. Beyond its direct application in HD-tDCS, this insight opens the door for alternative neuromodulation strategies, such as neurofeedback training, where individuals could learn to self-regulate network activity to reduce CS susceptibility. Future protocols may further exploit brain plasticity for long-term CS resistance, particularly when combined with adaptive exposure training. Practical applications extend to aviation, military, medical simulation, and gaming, where prolonged XR immersion is required. Additionally, the SNN-based model offers a real-time, low-power predictive tool, paving the way for wearable or implantable neuromorphic solutions. Future research should explore longitudinal neuromodulation effects, individualized strategies, neurofeedback applications, and integration with VR motion adaptation techniques. By linking predictive biomarkers to functional modulation, this study advances both CS prevention strategies and broader neuromodulation approaches, contributing to the development of next-generation XR usability solutions.

Appendix

See the Tables 3 and 4.

Table 3 The VIMSSQ

Q1. How often have you experienced each of the following symptoms when using any of these devices? (circle your response)				
Nausea	*Never*	*Rarely*	*Sometimes*	*Often*
Headache	*Never*	*Rarely*	*Sometimes*	*Often*
Dizziness	*Never*	*Rarely*	*Sometimes*	*Often*
Fatigue	*Never*	*Rarely*	*Sometimes*	*Often*
Eye-strain	*Never*	*Rarely*	*Sometimes*	*Often*
Q2. Have any of these symptoms **stopped** you using any of these devices or made you **avoid** viewing such displays? (circle your response)				
	Never	*Rarely*	*Sometimes*	*Often*
Q3. If you have answered stopped or avoided, please list the devices or displays that you avoid				

This questionnaire is designed to measure your experience with different visual display or entertainment devices and if they ever caused discomfort. Visual display or entertainment devices include Movie Theatre or Cinema, Smartphones and Tablets with movies or games, Video games, Virtual Reality Glasses or Head Mounted Displays, Simulators, Large Public Moving Display Advertising or Information Screens. Please answer these questions solely with respect to your experiences during adulthood (older than 18 years) and ignore childhood experiences

Table 4 The VRSQ

VRSQ symptom	Oculomotor	Disorientation
Virtual reality sickness questionnaire (VRSQ)		
1. General discomfort	O	
2. Fatigue	O	
3. Eyestrain	O	
4. Difficulty focusing	O	
5. Headache		O
6. Fullness of head		O
7. Blurred vision		O
8. Dizzy (eyes closed)		O
9. Vertigo		O
Total	[1]	[2]
SSQ components	Computation	
Computation score of VRSQ		
Oculomotor	([1]/12)*100	
Disorientation	([2]/15)*100	
Total	(Oculomotor score + Disorientation score)/2	

Acknowledgements The authors wish to acknowledge the team at Neuroelectrics for the brain modelling.

Author contributions Conceptualization: A.H.X.Y and Y.O.C. Methodology: A.H.X.Y., Y.O.C and N.K. Data curation: A.H.X.Y. Data collection: A.H.X.Y. Data Analysis: A.H.X.Y and C. G-A. Data Analysis Review: Y.O.C. and N.K. First draft of the paper: A.H.X.Y. Final Version: All authors; Supervision: Y.O.C. and N.K. Funding: Y.O.C. All authors read and approved the final manuscript.

Funding Open access funding provided by The University of Otago. Funding by Yusuf Cakmak's PBRF grant.

Data availability Data is not available based on the ethical approval that limits the secondary usage/sharing of the data.

Declarations

Ethical approval This study was approved by the University of Otago Human Ethics Committee (H22/016) and performed in accordance with relevant guidelines and regulations. The study is also retrospectively registered to ANZCTR with a clinical trial no: ACTRN12623000941662.

Competing interests The authors declare no competing interests.

References

Adriana Cárdenas-Robledo L, Hernández-Uribe Ó, Reta C, Antonio Cantoral-Ceballos J (2022) Extended reality applications in industry 4.0—a systematic literature review. Telemat Inform 73:101863. https://doi.org/10.1016/j.tele.2022.101863

Arshad Q, Cerchiai N, Goga U et al (2015) Electrocortical therapy for motion sickness. Neurology 85:1257–1259. https://doi.org/10.1212/WNL.0000000000001989

Ball C, Huang K-T, Francis J (2021) Virtual reality adoption during the COVID-19 pandemic: a uses and gratifications perspective. Telematics Inform 65:101728. https://doi.org/10.1016/j.tele.2021.101728

Batsikadze G, Moliadze V, Paulus W et al (2013) Partially non-linear stimulation intensity-dependent effects of direct current stimulation on motor cortex excitability in humans. J Physiol 591:1987–2000. https://doi.org/10.1113/jphysiol.2012.249730

Bergmann TO (2018) Brain state-dependent brain stimulation. Front Psychol. https://doi.org/10.3389/fpsyg.2018.02108

Bestmann S, de Berker AO, Bonaiuto J (2015) Understanding the behavioural consequences of noninvasive brain stimulation. Trends Cogn Sci 19:13–20. https://doi.org/10.1016/j.tics.2014.10.003

Bikson M, Grossman P, Thomas C et al (2016) Safety of transcranial direct current stimulation: evidence based update 2016. Brain Stimul 9:641–661. https://doi.org/10.1016/j.brs.2016.06.004

Brainard A, Gresham C (2014) Prevention and treatment of motion sickness. Am Fam Physician 90(1):41–46.

Bronstein AM, Patel M, Arshad Q (2015) A brief review of the clinical anatomy of the vestibular-ocular connections—how much do we know? Eye 29(2):163–170. https://doi.org/10.1038/eye.2014.262

Brown P, Spronck P, Powell W (2022) The simulator sickness questionnaire, and the erroneous zero baseline assumption. Front Virtual Real 3:945800. https://doi.org/10.3389/frvir.2022.945800

Brunoni AR, Amadera J, Berbel B et al (2011) A systematic review on reporting and assessment of adverse effects associated with transcranial direct current stimulation. Int J Neuropsychopharmacol 14:1133–1145. https://doi.org/10.1017/S1461145710001690

Burkitt AN (2006) A review of the integrate-and-fire neuron model: I. Homogeneous synaptic input. Biol Cybern 95:1–19

Caserman P, Garcia-Agundez A, Gámez Zerban A, Göbel S (2021) Cybersickness in current-generation virtual reality

head-mounted displays: systematic review and outlook. Virtual Real 25:1153–1170
Cassani R, Novak GS, Falk TH, Oliveira AA (2020) Virtual reality and non-invasive brain stimulation for rehabilitation applications: a systematic review. J Neuroeng Rehabil 17:147. https://doi.org/10.1186/s12984-020-00780-5
Cesari V, Orrù G, Piarulli A et al (2024) The effects of right temporo-parietal junction stimulation on embodiment, presence, and performance in teleoperation. AIMS Neurosci 11:352–373. https://doi.org/10.3934/Neuroscience.2024022
Cheung BS, Heskin R, Hofer KD (2003) Failure of cetirizine and fexofenadine to prevent motion sickness. Ann Pharmacother 37:173–177
Cipresso P, Giglioli IAC, Raya MA, Riva G (2018) The past, present, and future of virtual and augmented reality research: a network and cluster analysis of the literature. Front Psychol 9:2086. https://doi.org/10.3389/fpsyg.2018.02086
Coffman BA, Clark VP, Parasuraman R (2014) Battery powered thought: enhancement of attention, learning, and memory in healthy adults using transcranial direct current stimulation. Neuroimage 85:895–908
Dagan M, Herman T, Harrison R et al (2018) Multitarget transcranial direct current stimulation for freezing of gait in Parkinson's disease. Mov Disord 33:642–646. https://doi.org/10.1002/mds.27300
DaSilva AF, Truong DQ, DosSantos MF, Toback RL, Datta A, Bikson M (2015) State-of-art neuroanatomical target analysis of high-definition and conventional tDCS montages used for migraine and pain control. Front Neuroanat 9:89. https://doi.org/10.3389/fnana.2015.00089
De Ridder D, Vanneste S, Weisz N, Londero A, Schlee W, Elgoyhen AB, Langguth B (2014) An integrative model of auditory phantom perception: tinnitus as a unified percept of interacting separable subnetworks. Neurosci Biobehav Rev 44:16–32. https://doi.org/10.1016/j.neubiorev.2013.03.021
Dennison MS, Wisti AZ, D'Zmura M (2016) Use of physiological signals to predict cybersickness. Displays 44:42–52. https://doi.org/10.1016/j.displa.2016.07.002
Feldman DE (2012) The spike-timing dependence of plasticity. Neuron 75:556–571. https://doi.org/10.1016/j.neuron.2012.08.001
Feltman KA, Hayes AM, Bernhardt KA et al (2019) Viability of tDCS in military environments for performance enhancement: a systematic review. Mil Med 185:53–60. https://doi.org/10.1093/milmed/usz189
Fertonani A, Miniussi C (2017) Transcranial electrical stimulation: what we know and do not know about mechanisms. Neuroscientist 23:109–123. https://doi.org/10.1177/1073858416631966
Frank SM, Baumann O, Mattingley JB, Greenlee MW (2014) Vestibular and visual responses in human posterior insular cortex. J Neurophysiol 112:2481–2491. https://doi.org/10.1152/jn.00078.2014
Galili E, Averbuch Zehavi E, Zadik Y, Caspi T, Meltzer L, Merdler I, Kuten J, Tal D (2019) Long-term scopolamine treatment and dental caries. Clin Oral Investig 23(5):2339–2344. https://doi.org/10.1007/s00784-018-2688-3
Geuzaine C, Remacle J-F (2009) Gmsh: A 3-D finite element mesh generator with built-in pre- and post-processing facilities. Int J Numer Methods Eng 79:1309–1331. https://doi.org/10.1002/nme.2579
Golding JF, Rafiq A, Keshavarz B (2021) Predicting individual susceptibility to visually induced motion sickness by questionnaire. Front Virtual Real 2(3):576871. https://doi.org/10.3389/frvir.2021.576871
Hampstead BM, Brown GS, Hartley JF (2014) Transcranial direct current stimulation modulates activation and effective connectivity during spatial navigation. Brain Stimul 7(2):314–324. https://doi.org/10.1016/j.brs.2013.12.006
Hulme SR, Jones OD, Abraham WC (2013) Emerging roles of metaplasticity in behaviour and disease. Trends Neurosci 36:353–362. https://doi.org/10.1016/j.tins.2013.03.007
Ivanov D, Chezhegov A, Kiselev M et al (2022) Neuromorphic artificial intelligence systems. Front Neurosci 16:959626. https://doi.org/10.3389/fnins.2022.959626
Jacobson L, Koslowsky M, Lavidor M (2012) tDCS polarity effects in motor and cognitive domains: a meta-analytical review. Exp Brain Res 216:1–10. https://doi.org/10.1007/s00221-011-2891-9
Jiang M, Dimitriadis S, Seet MS et al (2022) Multilayer network framework reveals cross-frequency coupling hubs in cortical olfactory perception. Annu Int Conf IEEE Eng Med Biol Soc 2022:3338–3341. https://doi.org/10.1109/EMBC48229.2022.9871445
Karrim N, Magula N, Saman Y (2017) Antihistamines for motion sickness. Cochrane Database Syst Rev 2017:012715. https://doi.org/10.1002/14651858.CD012715
Kasabov NK (2014) NeuCube: a spiking neural network architecture for mapping, learning and understanding of spatio-temporal brain data. Neural Netw 52:62–76. https://doi.org/10.1016/j.neunet.2014.01.006
Kasabov NK (2018) Time-space, spiking neural networks and brain-inspired artificial intelligence (Springer Series on Bio- and Neurosystems). Springer Publishing Company, Inc
Kasabov N, Scott N, Tu E et al (2016) Design methodology and selected applications of evolving spatio-temporal data machines in the NeuCube neuromorphic framework. Neural Netw 78:1–14
Kennedy RS, Lane NE, Berbaum KS, Lilienthal MG (1993) Simulator sickness questionnaire: an enhanced method for quantifying simulator sickness. Int J Aviat Psychol 3(3):203–220. https://doi.org/10.1207/s15327108ijap0303_3
Keshavarz B, Hecht H (2011) Validating an efficient method to quantify motion sickness. Hum Factors 53(4):415–426. https://doi.org/10.1177/0018720811403736
Kim A, Lee JE, Lee KM (2023) Exploring the relative effects of body position and locomotion method on presence and cybersickness when navigating a virtual environment. ACM Trans Appl Percept 21:1–25. https://doi.org/10.1145/3627706
Koch A, Cascorbi I, Westhofen M, Dafotakis M, Klapa S, Kuhtz-Buschbeck JP (2018) The neurophysiology and treatment of motion sickness. Deutsches Arztebl Int 115(41):687–696. https://doi.org/10.3238/arztebl.2018.0687
Koessler L, Maillard L, Benhadid A et al (2009) Automated cortical projection of EEG sensors: anatomical correlation via the international 10–10 system. Neuroimage 46:64–72. https://doi.org/10.1016/j.neuroimage.2009.02.006
Kohl RL, Homick JL, Cintron N, Calkins DS (1987) Lack of effects of astemizole on vestibular ocular reflex, motion sickness, and cognitive performance in man. Aviat Space Environ Med 58:1171–1174
Krokos E, Varshney A (2021) Quantifying VR cybersickness using EEG. Virtual Real. https://doi.org/10.1007/s10055-021-00517-2
Lacko D, Vleugels J, Fransen E et al (2017) Ergonomic design of an EEG headset using 3D anthropometry. Appl Ergon 58:128–136. https://doi.org/10.1016/j.apergo.2016.06.002
Langbehn E, Steinicke F, Koo-Poeggel P et al (2019) Stimulating the brain in VR: effects of transcranial direct-current stimulation on redirected walking. In: ACM symposium on applied perception
Lee Y, Lai HY, Lin PC, Huang SJ, Lin YS (2003) Dexamethasone prevents postoperative nausea and vomiting more effectively in women with motion sickness. Can J Anaesth 50(3):232–237. https://doi.org/10.1007/BF03017790
Leung AK, Hon KL (2019) Motion sickness: an overview. Drugs Context 8. https://doi.org/10.7573/dic.2019-9-4
Li G, Varela FM, Habib A, Zhang Q, McGill M, Brewster S, Pollick F (2020) Exploring the feasibility of mitigating VR-HMD-induced

cybersickness using cathodal transcranial direct current stimulation. In: Proceedings of the 2020 IEEE international conference on Artificial Intelligence and Virtual Reality (AIVR), 14–18 Dec 2020

Li G, Onuoha O, McGill M, Brewster S, Chen CP, Pollick F (2021) Decreased brain functional connectivity in VR users during cybersickness. In: Proceedings of the 3rd neuroergonomics conference

Luetje CM, Wooten J (1996) Clinical manifestations of transdermal scopolamine addiction. Ear Nose Throat J 75:210–214. https://doi.org/10.1177/014556139607500408

Makani A, Saryazdi R, Givetash S, Keshavarz B (2024) The presence of an avatar can reduce cybersickness in virtual reality. Virtual Real 28:163. https://doi.org/10.1007/s10055-024-01057-1

Martin N, Mathieu N, Pallamin N, et al (2020) Virtual reality sickness detection: an approach based on physiological signals and machine learning. In: 2020 IEEE international symposium on mixed and augmented reality. ISMAR, pp 387–399

Martirosov S, Bureš M, Zítka T (2022) Cyber sickness in low-immersive, semi-immersive, and fully immersive virtual reality. Virtual Real 26:15–32

Marzbani H, Marateb HR, Mansourian M (2016) Neurofeedback: a comprehensive review on system design, methodology and clinical applications. Basic Clin Neurosci 7:143–158. https://doi.org/10.15412/J.BCN.03070208

Mauri M, Rancati G, Riva G, Gaggioli A (2024) Comparing the effects of immersive and non-immersive real estate experience on behavioral intentions. Comput Hum Behav 150:107996. https://doi.org/10.1016/j.chb.2023.107996

Miranda PC, Mekonnen A, Salvador R, Ruffini G (2013) The electric field in the cortex during transcranial current stimulation. Neuroimage 70:48–58. https://doi.org/10.1016/j.neuroimage.2012.12.034

Mohan A, De Ridder D, Vanneste S (2016) Emerging hubs in phantom perception connectomics. Neuroimage Clin 11:181–194. https://doi.org/10.1016/j.nicl.2016.01.022

Noreen S, Maqbool I, Madni A (2021) Dexamethasone: therapeutic potential, risks, and future projection during COVID-19 pandemic. Eur J Pharmacol 894:173854. https://doi.org/10.1016/j.ejphar.2021.173854

Opitz A, Paulus W, Will S et al (2015) Determinants of the electric field during transcranial direct current stimulation. Neuroimage 109:140–150. https://doi.org/10.1016/j.neuroimage.2015.01.033

Ostrowski J, Svaldi J, Schroeder PA (2022) More focal, less heterogeneous? Multi-level meta-analysis of cathodal high-definition transcranial direct current stimulation effects on language and cognition. J Neural Transm (Vienna) 129:861–878. https://doi.org/10.1007/s00702-022-02507-3

Padmanaban N, Ruban T, Sitzmann V et al (2018) Towards a machine-learning approach for sickness prediction in 360° stereoscopic videos. IEEE Trans Visual Comput Graph. https://doi.org/10.1109/TVCG.2018.2793560

Palmisano S, Constable R (2022) Reductions in sickness with repeated exposure to HMD-based virtual reality appear to be game-specific. Virtual Real. https://doi.org/10.1007/s10055-022-00634-6

Rahimi MD, Fadardi JS, Saeidi M et al (2020) Effectiveness of cathodal tDCS of the primary motor or sensory cortex in migraine: a randomized controlled trial. Brain Stimul 13:675–682. https://doi.org/10.1016/j.brs.2020.02.012

Raiser TM, Flanagin VL, Duering M et al (2020) The human corticocortical vestibular network. Neuroimage 223:117362. https://doi.org/10.1016/j.neuroimage.2020.117362

Rebenitsch L, Owen C (2016) Review on cybersickness in applications and visual displays. Virtual Real 20(2):101–125. https://doi.org/10.1007/s10055-016-0285-9

Ruffini G, Fox MD, Ripolles O et al (2014) Optimization of multifocal transcranial current stimulation for weighted cortical pattern targeting from realistic modeling of electric fields. Neuroimage 89:216–225. https://doi.org/10.1016/j.neuroimage.2013.12.002

Salvador R, Biagi MC, Puonti O, et al (2021) Personalization of multi-electrode setups in tCS/tES: methods and advantages. In: Makarov SN, Noetscher GM, Nummenmaa A (eds) Brain and human body modeling 2020: computational human models presented at EMBC 2019 and the BRAIN initiative® 2019 meeting. Springer, pp 119–135

Scheurer ME, El-Zein R, Thompson PA et al (2008) Long-term anti-inflammatory and antihistamine medication use and adult glioma risk. Cancer Epidemiol Biomarkers Prev 17:1277–1281. https://doi.org/10.1158/1055-9965.Epi-07-2621

Schmäl F (2013) Neuronal mechanisms and the treatment of motion sickness. Pharmacology 91:229–241. https://doi.org/10.1159/000350185

Shiravand F, Motamedi P, Amani-Shalamzari S et al (2024) Effect of repeated sessions of transcranial direct current stimulation on subjective and objective measures of recovery and performance in soccer players following a soccer match simulation. Sci Rep 14:20809. https://doi.org/10.1038/s41598-024-71701-y

Siebner HR, Lang N, Rizzo V et al (2004) Preconditioning of low-frequency repetitive transcranial magnetic stimulation with transcranial direct current stimulation: evidence for homeostatic plasticity in the human motor cortex. J Neurosci 24:3379–3385. https://doi.org/10.1523/JNEUROSCI.5316-03.2004

Smith JL, Trofimova A, Ahluwalia V et al (2022) The "vestibular neuromatrix": a proposed, expanded vestibular network from graph theory in post-concussive vestibular dysfunction. Hum Brain Mapp 43:1501–1518. https://doi.org/10.1002/hbm.25737

Souchet AD, Lourdeaux D, Burkhardt J-M, Hancock PA (2023) Design guidelines for limiting and eliminating virtual reality-induced symptoms and effects at work: a comprehensive, factor-oriented review. Front Psychol. https://doi.org/10.3389/fpsyg.2023.1161932

Spinks A, Wasiak J (2011) Scopolamine (hyoscine) for preventing and treating motion sickness. The Cochrane Database of Systematic Reviews 2011:002851. https://doi.org/10.1002/14651858.CD002851.pub4

Stanney K, Lawson BD, Rokers B et al (2020) Identifying causes of and solutions for cybersickness in immersive technology: reformulation of a research and development agenda. Int J Hum Comput Interact 36:1783–1803. https://doi.org/10.1080/10447318.2020.1828535

Sullivan GM, Feinn R (2012) Using effect size—or why the p value is not enough. J Grad Med Educ 4(3):279–282. https://doi.org/10.4300/jgme-d-12-00156.1

Takeuchi N, Mori T, Suzukamo Y, Izumi S-I (2018) Modulation of excitability in the temporoparietal junction relieves virtual reality sickness. Cyberpsychol Behav Soc Netw 21(6):381–387. https://doi.org/10.1089/cyber.2017.0499

Tauscher J-P, Witt A, Bosse S et al (2020) Exploring neural and peripheral physiological correlates of simulator sickness. Comput Anim Virtual Worlds 31:1953. https://doi.org/10.1002/cav.1953

Thair H, Holloway AL, Newport R, Smith AD (2017) Transcranial Direct Current Stimulation (tDCS): a beginner's guide for design and implementation. Front Neurosci 11:641. https://doi.org/10.3389/fnins.2017.00641

Thielscher A, Antunes A, Saturnino GB (2015) Field modeling for transcranial magnetic stimulation: a useful tool to understand the physiological effects of TMS? Annu Int Conf IEEE Eng Med Biol Soc 2015:222–225. https://doi.org/10.1109/EMBC.2015.7318340

To WT, Eroh J, Hart J, Vanneste S (2018) Exploring the effects of anodal and cathodal high definition transcranial direct current stimulation targeting the dorsal anterior cingulate cortex. Sci Rep 8:4454. https://doi.org/10.1038/s41598-018-22730-x

Toschi N, Kim J, Sclocco R, Duggento A, Barbieri R, Kuo B, Napadow V (2017) Motion sickness increases functional connectivity between visual motion and nausea-associated brain regions. Auton Neurosci 202:108–113. https://doi.org/10.1016/j.autneu.2016.10.003

Vanneste S, De Ridder D (2012) The auditory and non-auditory brain areas involved in tinnitus. An emergent property of multiple parallel overlapping subnetworks. Front Syst Neurosci 6:31. https://doi.org/10.3389/fnsys.2012.00031

Vega-Zuniga T, Sumser A, Symonova O et al (2025) A thalamic hub-and-spoke network enables visual perception during action by coordinating visuomotor dynamics. Nat Neurosci. https://doi.org/10.1038/s41593-025-01874-w

Voneida TJ (1998) Sperry's concept of mind as an emergent property of brain function and its implications for the future of humankind. Neuropsychologia 36:1077–1082. https://doi.org/10.1016/s0028-3932(98)00061-x

Wallace D, Cooper NR, Paulmann S et al (2016) Perceived comfort and blinding efficacy in randomised sham-controlled transcranial direct current stimulation (tDCS) trials at 2 mA in young and older healthy adults. PLoS ONE 11:0149703. https://doi.org/10.1371/journal.pone.0149703

Woods AJ, Antal A, Bikson M et al (2016) A technical guide to tDCS, and related non-invasive brain stimulation tools. Clin Neurophysiol 127:1031–1048. https://doi.org/10.1016/j.clinph.2015.11.012

Yang AHX, Kasabov NK, Cakmak YO (2023) Prediction and detection of virtual reality induced cybersickness: a spiking neural network approach using spatiotemporal EEG brain data and heart rate variability. Brain Informatics 10:15. https://doi.org/10.1186/s40708-023-00192-w

Zheng Y, Wang XL, Mo FF, Li M (2014) Dexamethasone alleviates motion sickness in rats in part by enhancing the endocannabinoid system. Eur J Pharmacol 727:99–105. https://doi.org/10.1016/j.ejphar.2014.01.047